High-order wave directionality and topological valley modes in elastic quasicrystals

D. Beli [1], **M. I. N. Rosa** [2], **C. De Marqui Jr.** [1], **M. Ruzzene** [2]
[1] University of Sao Paulo, Sao Carlos School of Engineering,
Sao Carlos SP 13563-120, Brazil
email: **dbeli@usp.br**

[2] University of Colorado Boulder, Department of Mechanical Engineering,
Boulder CO 80309, Colorado, USA

Abstract
The spatial design of phononic crystals and acoustic-elastic metamaterials is based on translational periodicity and, hence, their wave phenomena, such as the directionality and topological guiding, are restricted to the crystallographic symmetries (e.g., 2-, 4- and 6-fold). This conference paper summarizes our recent efforts on expanding the wave manipulation possibilities (e.g., directionality and topological guiding) of architected materials to quasicrystals exhibiting higher order rotational symmetries, such as 10-fold. They open new possibilities for wave applications such as focusing, sensing, guiding and imaging beyond the symmetries provided by the periodic configurations.

1 Introduction

Phononic crystals and acoustic-elastic metamaterials are traditionally based on translational periodicity, and hence, their wave directionality phenomena as well as their topological waveguide features are restricted to the crystallographic symmetries (e.g., 2-, 4- and 6-fold) [1, 2, 3, 4]. This conference paper summarizes our recent efforts on expanding the wave manipulation possibilities of architected materials to quasicrystals exhibiting higher order rotational symmetries, such as 5-, 8- and 10-fold [5, 6, 7]. This work outlines powerful tools as well as highlights the rich underlying physics behind the wave phenomena in quasicrystalline architected materials. It opens new possibilities for applications involving the unusual wave front directivity with high-order symmetry, such as focusing, sensing, and imaging beyond the symmetries provided by the periodic configurations. Moreover, these results expand the possibilities of robust topological wave transport to the so far largely unexplored symmetries of quasicrystals, which may pave the way to novel applications and devices. This paper is organized as follows: following this introduction, Section 2 describes the design of the quasicrystalline plates. Next, section 3 describes the dispersion properties and wave directionality results, followed by the topological valley modes in section 4. Section 5 summarizes the main contributions of this work.

2 Quasicrystal design

The strategy to design the quasiperiodic elastic metamaterial plates is based on the geometric representation in 2D wave number space [8, 5]. A continuum distribution in physical space $\phi(\mathbf{r})$, with $\mathbf{r} = [x, y] \in \mathcal{R}^2$, is defined by directly assigning N Bragg peaks in reciprocal space ($\mathbf{k} = [k_x, k_y] \in \mathcal{R}^2$) as points in the two-dimensional Fourier spectra. These Bragg peaks are angularly spaced by $\theta_N = 2\pi/N$ over a circle of fundamental wave number k_0. In this work, only even number of peaks is considered to guarantee a real

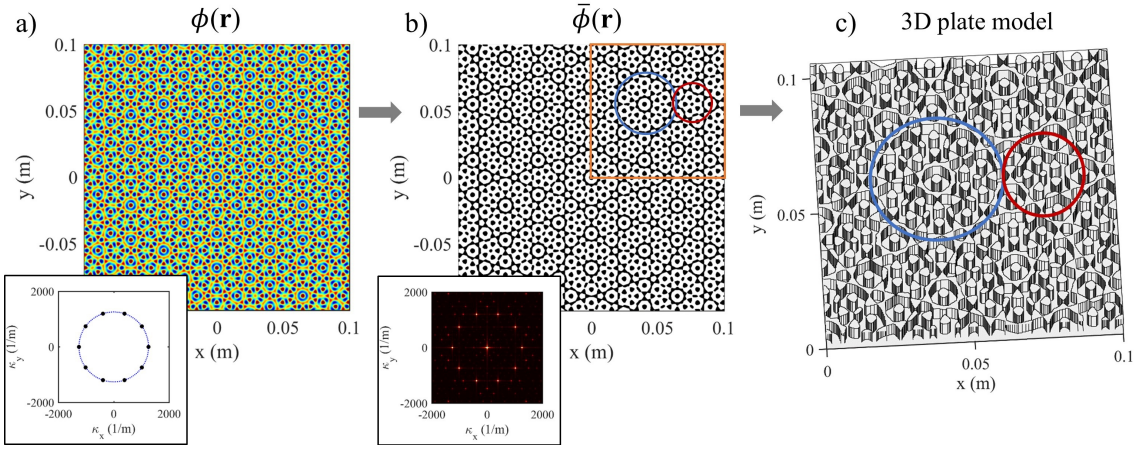

Figure 1: Design strategy for the 10-fold quasicrystal plate with $\texttt{vf} = 0.30$: two-dimensional physical distribution by assigning 10 Bragg peaks (a), two-phase distribution after applying the threshold procedure and its Fourier transform (i.e., diffraction pattern) (b): phase `A` (white) and phase `B` (black). Three-dimensional quasiperiodic plate obtained by extruding phase `B` towards z direction, which produces the geometry in (c). Adapted from Beli et al. [6].

distribution in physical space. Therefore, reciprocal and physical spaces can be expressed, respectively, as:

$$\hat{\phi}(\mathbf{k}) = \sum_{n=0}^{N-1} \delta(\mathbf{k} - \mathbf{k}_n), \quad \text{and} \quad \phi(\mathbf{r}) = \sum_{n=0}^{N-1} e^{\mathrm{i}\mathbf{k}_n \cdot \mathbf{r}}, \tag{1}$$

where δ is the delta function that locates the wave number $\mathbf{k}_n$ of each Bragg peak; moreover, $\mathbf{k}_n = k_0[\cos(n\theta_N), \sin(n\theta_N)]$, with $n = 0, ..., N-1$ and $k_0 = 2\pi/\lambda_0$ is the radius of the design circle in reciprocal space, where λ_0 is the fundamental wavelength. In this design strategy, a single parameter N defines the rotational symmetry of the distribution in physical space, which leads to periodic distributions (1D bilayer for $N = 2$, square pattern for $N = 4$ and hexagonal pattern for $N = 6$) or quasiperiodic distributions with rotationally N-fold symmetry such as the 8-fold and 10-fold.

For practical implementations in elastic continuum structures, a two-phase distribution is desirable, and hence, a threshold procedure is applied to the real continuum field. This new distribution $\bar{\phi}(\mathbf{r})$ assumes only two phases, which are produced by comparing the local field level to a chosen level $\bar{\phi}_0$: a phase `A` (white) is defined for $\phi(\mathbf{r}) \leq \bar{\phi}_0$ and a phase `B` (black) is defined for $\phi(\mathbf{r}) > \bar{\phi}_0$. Based on the phase ratio, a volume (or filling) fraction is defined by $\texttt{vf} = v_{\texttt{B}}/(v_{\texttt{A}} + v_{\texttt{B}})$. Herein, the metamaterial plate is designed using a single material with geometric thickness modulation given by $\bar{\phi}(\mathbf{r})$, where a flat plate (phase `A`) is partially covered in one side by pillars (phase `B`). Figure 1 summarizes the design process, from the choice of Bragg peaks in the reciprocal space to the three-dimensional plate with 10-fold symmetry and $\texttt{vf} = 0.30$. Reference [5] details this design strategy for other fold symmetries and volume fractions considering 2D domains with material phase modulation and in-plane wave behavior, i.e. steps (a-b) on Fig. 1.

3 Wave directionality

The dispersion properties are used to understand and predict the dynamic behavior of phononic and metamaterial structures related to wave propagation and manipulation. For periodic materials, the band structure is obtained by enforcing Bloch conditions on the unit cell boundaries. However, Bloch-Floquet theory cannot be applied to the present quasicrystalline plates due to their lack of translational periodicity. Instead, we rely on transient wave-fields $\mathbf{u}(x, y, t)$, and their correspondent 3D-FT (Fourier transform) $\hat{\mathbf{U}}(k_x, k_y, \omega)$, to estimate the dispersion properties of the quasicrystalline plates.

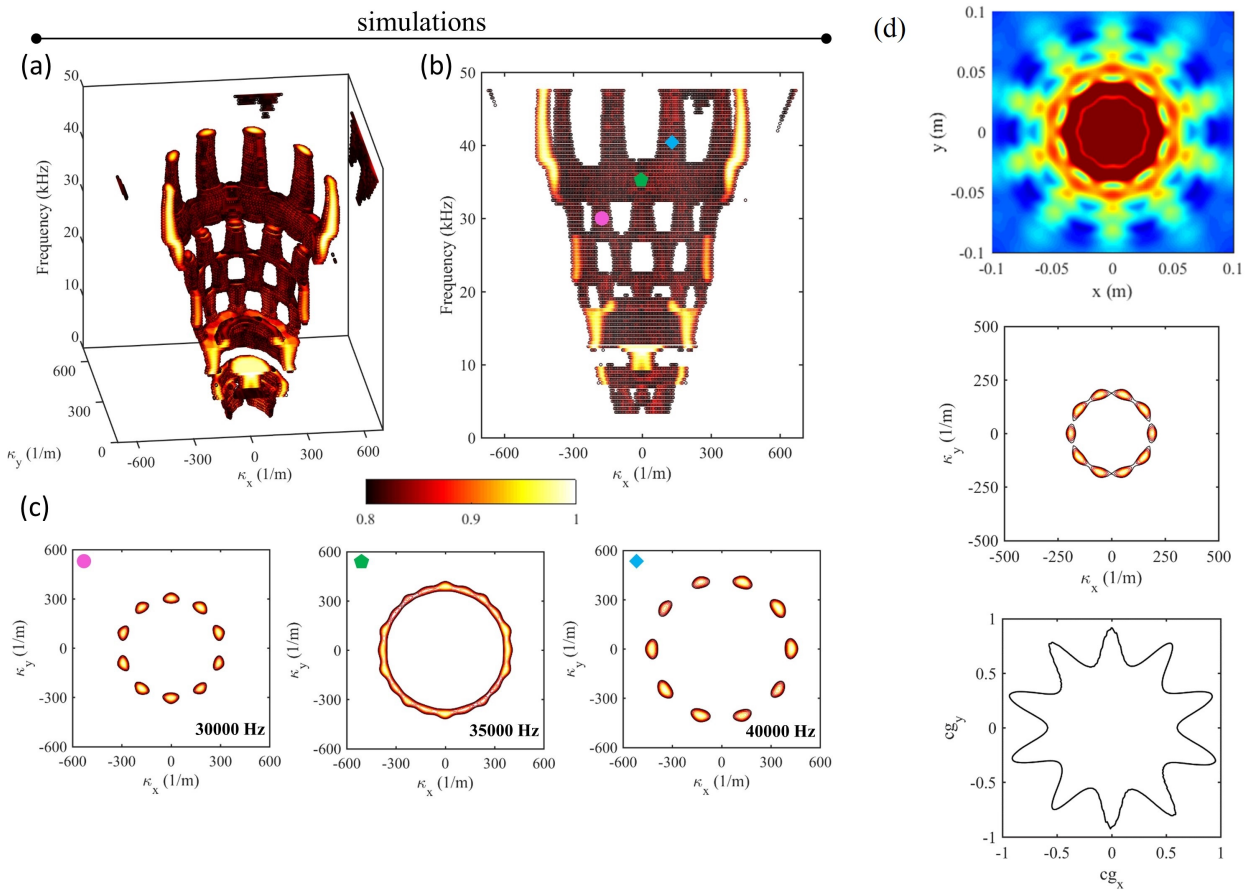

Figure 2: Approximated dispersion surface of the 10-fold quasicrystal plate obtained by 3D Fourier transform of the time response: 3D view (a), sectional view on $\kappa_x\omega$ plane (b), and contours at specific frequencies showing the transition between two bands twisted by $\theta_N/2$ (c). Directional wave behavior for the 10-fold metamaterial plate at 9.3 kHz (d): the first row corresponds to the RMS of the wave field averaging across all time, the second row corresponds to the RMS of the wave number contours averaging across all frequencies, and the third row corresponds to the estimated group velocity contour at the center frequency. Adapted from Beli et al. [6].

The dispersion behavior of the quasicrystalline plates is exemplified by using the 10-fold case (i.e., $N = 10$), whose the results are summarized in Fig. 2. The dispersion surfaces for the flexural waves are characterized by a 10-fold rotational symmetry that manifests throughout the majority of the bands, as highlighted by the contours displayed for selected frequencies. In particular, several bands of highly anisotropic contours are identified, which are characterized by 10 separated peaks of high amplitude in reciprocal space forming the 10-fold symmetry. We note that the rotational symmetry twists by $\theta_N/2 = 18^{\text{o}}$ in certain frequency ranges shown in Fig. 2(b), for example around 22, 26 and 35 kHz. This behavior highlights how the dispersion properties of the quasicrystalline plates are characterized by several bands that preserve the N-fold symmetry of the design, and may present different anisotropy directions. Specifically, at 9.3kHz the waves propagate preferentially along 10 symmetric directions in a wave-beaming fashion as shown in Fig. 2(d). The Fourier transform shows 10 Fourier peaks that characterize such behavior, while the group velocity further confirms the preferential directions of wave propagation.

The effects of directionality provided by the higher order symmetries on the wave diffraction are also illustrated. For this purpose, the upper half of the quasicrystal domain considered in the previous section (10-fold, $x = [-0.1,\ 0.1]$ m and $y = [0,\ 0.2]$ m) is combined to an uniform plate ($x = [-0.1,\ 0.1]$ m and $y = [-0.075,\ 0]$ m) with constant thickness h_{U} = 4 mm. A line-source excitation is centered at the bottom of the uniform plate ($x = 0$ and $y = -0.075$ m), so that the incident wave propagates along the

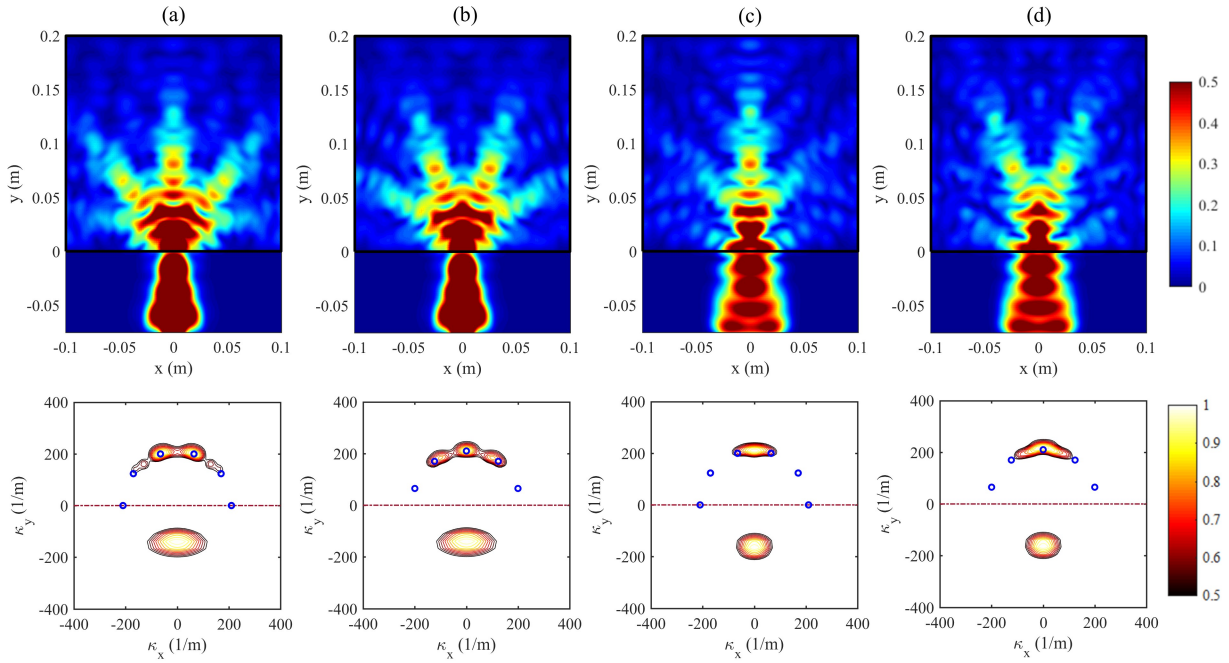

Figure 3: Wave diffraction at 9.3 kHz in a half of the extended 10-fold quasiperiodic metamaterial plate, where the incident wave with width $b_s = 0.02$ m (a-b) or $b_s = 0.06$ m (c-d) are aligned $\theta = 0$ (a, c) or twisted by $\theta = \theta_N/2$ (b, d) in relation to one of the Bragg peaks in reciprocal space at 9.3 kHz (first line). The top line depicts the RMS of the displacement field averaging across all time and the bottom line the correspondent RMS of the wave number contour averaging across all frequencies: $\kappa_y > 0$ for the quasicrystal plate and $\kappa_y < 0$ for the uniform plate. Diffraction patterns with focusing from one to four branches have been created. Adapted from Beli et al. [6].

positive y direction until it reaches the interface with the quasicrystalline domain ($y = 0$). The diffraction is illustrated by employing an excitation frequency of 9.3kHz, corresponding to the beaming behavior reported in Fig. 2(d). The results are summarized in Fig. 3 for different conditions that showcase different possible scenarios; the top row displays the RMS of the wave-field, while the bottom row displays the RMS of the reciprocal space content (the upper half, $\kappa_y > 0$, corresponding to the waves propagating in the quasicrystal, and the bottom half, $\kappa_y < 0$, corresponding to the incident wave in the homogeneous plate). The results in (a,b) correspond to a narrow line source of width 20 mm, which provides a broad wave number content for κ_x for the incident wave, while in (c,d) a wider line source of 60 mm produces an incident wave with narrower wave number content for κ_x. These different conditions are selected to illustrate a wealth of possibilities for wave diffraction that result in different numbers and orientations of directional branches propagating in the quasicrystalline plate, which can shift the wave behavior from beaming (i.e., multi-focal) to focusing (i.e., uni-focal) by controlling the quasicrystal orientation and the source width.

4 Topological valley modes

Next, we investigate the existence of topological valley-type waves in quasicrystalline structures. A design strategy similar to Section 2 is used to obtain the domains with distinct topological invariants. While the hexagonal lattice enables the construction of topological waveguides containing 60^o corners, the decagonal lattice allow sharp corners in the topological waveguides such as 36^o. The existence of valley states is well defined for periodic lattices; starting with the 6-fold symmetric lattice exhibiting Dirac cone degeneracy, 3-fold symmetric lattices with topological gaps characterized by opposite valley Chern numbers are obtained by breaking the inversion symmetry of the unit cell. This procedure is commonly defined as function of a

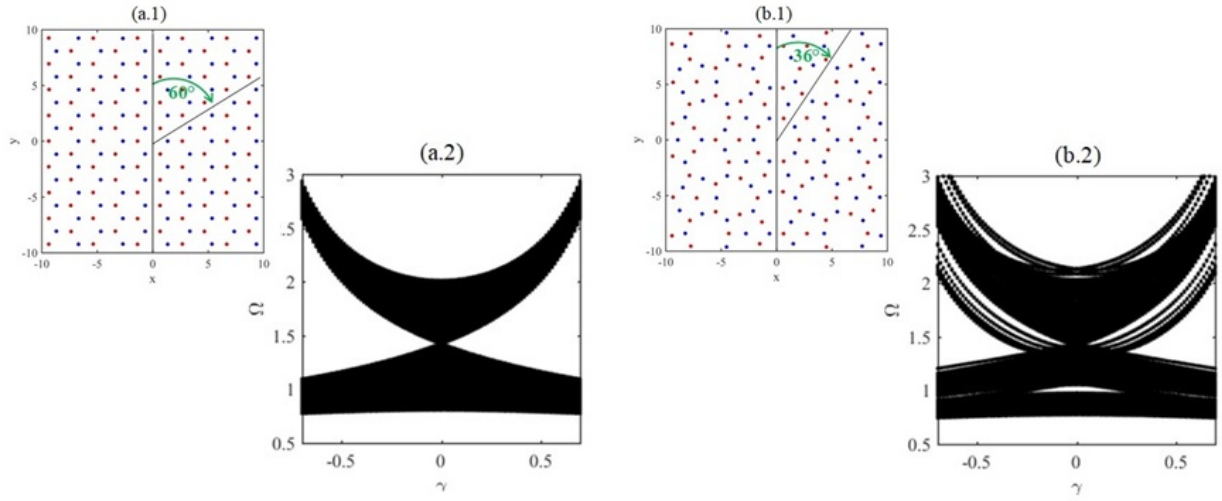

Figure 4: Hexagonal lattice (a.1) composed of two subsets of 3-fold lattices and the correspondent band inversion (a.2). Decagonal lattice (a.1) composed of two subsets of 5-fold lattices and the correspondent band inversion (a.2). The gaps close at $\gamma = 0$, the structures with gaps in opposite sides of the band inversion (i.e., $\gamma < 0$ and $\gamma > 0$) present distinct topological invariant.

single parameter (e.g., γ, which represents the mass modulation) that produces a band inversion as the gap closes and re-opens between the distinct 3-fold configurations with different topological properties as showin in Fig. 4(a). We extend this approach to 5-fold symmetric quasicrystals, where the band inversion is also observed as a function of a single parameter, with the band gap closure occurring for an intermediate 10-fold symmetric configuration as presented in Fig. 4(b). We observe the emergence of robust waves propagating along the interfaces between 5-fold symmetric domains of distinct topological properties (e.g., I and II) as shown in the time response simulation of Fig. 5. In particular, the higher order rotational symmetry of the quasicrystals allows for the design of unusual interfaces, since it provides more directions of angular symmetry then the periodic cases.

5 Conclusions

The spatial design of phononic crystals and acoustic-elastic metamaterials is based on translational periodicity, and hence, their wave phenomena, such as the directionality and topological guiding, are restricted to the crystallographic symmetries (e.g., 2-, 4- and 6-fold). In this work, the wave directionality as well as the topological valley states were expanded to high-order rotational symmetries, such as 10-fold, by employing quasiperiodic elastic metamaterial plates. Moreover, it opens new possibilities for applications involving the unusual wave front directivity and topological circuits with high-order symmetry (e.g., 10-fold), such as focusing, sensing, guiding and imaging beyond the symmetries provided by the periodic configurations.

Acknowledgements

D. Beli and C. De Marqui Jr. gratefully acknowledge the support from São Paulo Research Foundation (FAPESP) through grant reference numbers: 2018/18774-6, 2019/22464-5 and 2018/15894-0 (Research project - Periodic structure design and optimization for enhanced vibroacoustic performance: ENVIBRO). M. I. N. Rosa and M. Ruzzene gratefully acknowledge the support from the National Science Foundation (NSF) through the EFRI 1741685 grant and from the Army Research Office through grant W911NF-18-1-0036.

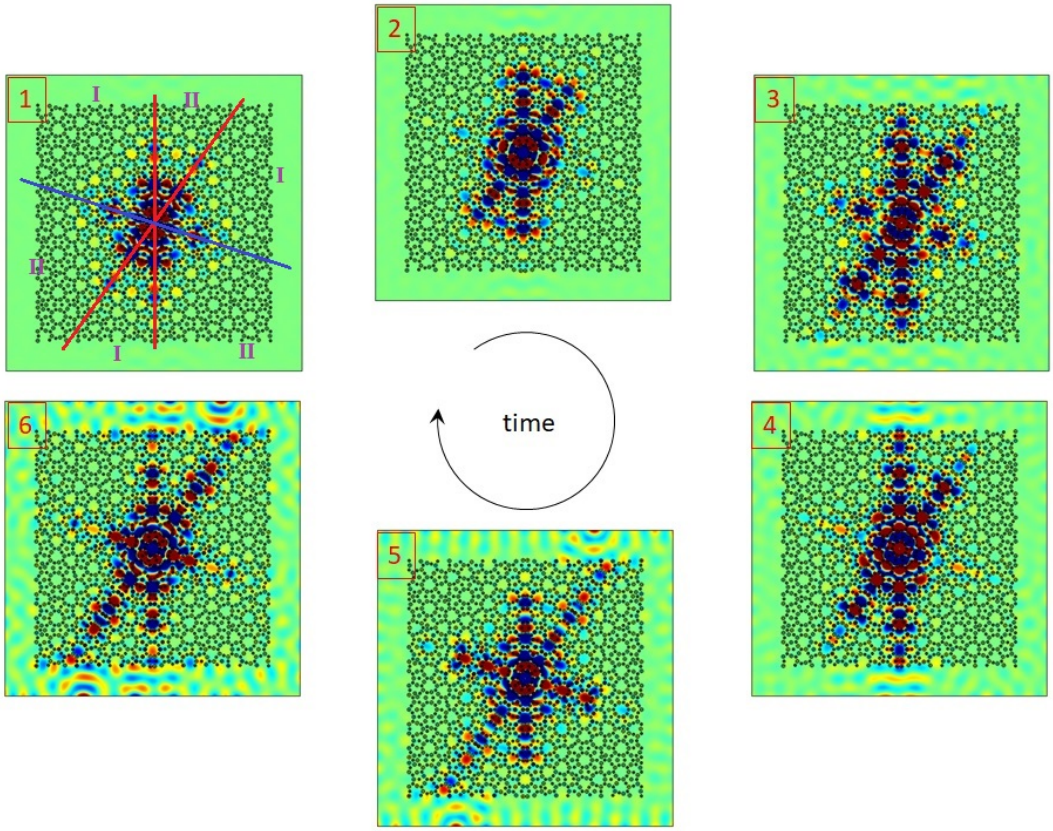

Figure 5: Time response simulation of a 10-fold quasicrystal plate with three topological interfaces, which were created by intercalating domains with opposite valley states, i.e. $\gamma < 0$ and $\gamma > 0$. The waves are guided through the topological interfaces while the bulk is isolated by the gaps.

References

[1] M. Ruzzene, F. Scarpa, and F. Soranna, "Wave beaming effects in two-dimensional cellular structures," *Smart Materials and Structures*, vol. 12, no. 3, 2003.

[2] M. Ruzzene and F. Scarpa, "Directional and band-gap behavior of periodic auxetic lattices," *Physica Status Solidi (B)*, vol. 242, no. 3, pp. 665-680, 2005.

[3] A. S. Phani, J. Woodhouse, and N. A. Fleck, "Wave propagation in two-dimensional periodic lattices," *The Journal of the Acoustical Society of America*, vol. 119, no. 4, pp. 1995-2005, 2006.

[4] S. Gonella and M. Ruzzene, "Analysis of in-plane wave propagation in hexagonal and re-entrant lattices," *Journal of Sound and Vibration*, vol. 312, no. 1-2, pp. 125-139, 2008.

[5] D. Beli, M. I. N. Rosa, C. De Marqui Jr and M. Ruzzene, "Mechanics and dynamics of two-dimensional quasicrystalline composites," *Extreme Mechanics Letters*, vol. 44, 101220, 2021.

[6] D. Beli, M. I. N. Rosa, C. De Marqui Jr and M. Ruzzene, "Wave beaming and diffraction in quasicrystalline elastic metamaterial plates," *arXiv preprint*, arXiv:2201.12270, 2022.

[7] D. Beli, M. I. N. Rosa, C. De Marqui Jr and M. Ruzzene, "Topological valley states in elastic quasicrystals," in *Proceedings of the aActive and Passive Smart Structures and Integrated Systems XVI*, Long Beach/CA, United States, 2022.

[8] T. Lubensky, *Chapter 6 - Symmetry, elasticity, and hydrodynamics in quasiperiodic structures, in Introduction to Quasicrystals, Aperiodicity and Order*, vol. 1, edited by M. V. Jari´c (Elsevier) pp. 199 – 280, 1988.